atmosphere

MDPI

Article

Hydrogeochemistry Characteristics of Groundwater in the Nandong Karst Water System, China

Xiuqun Zhu [1,2], Ling Liu [1,*], Funing Lan [2,*], Jun Li [3] and Shitian Hou [4]

[1] College of Hydrology and Water Resources, Hohai University, Nanjing 210098, China; zhuxq@hhu.edu.cn
[2] Institute of Karst Geology, Chinese Academy of Geological Sciences, Guilin 541004, China
[3] Hebei Key Laboratory of Water Quality Engineering and Comprehensive Utilization of Water Resources, Hebei University of Architecture, Zhangjiakou 075000, China; lipsgeology@karst.ac.cn
[4] Sinosteel Maanshan General Institute of Mining Research Co., Ltd., Maanshan 243000, China; 2120170016@email.cugb.edu.cn
* Correspondence: lingliu@hhu.edu.cn (L.L.); lfuning@karst.ac.cn (F.L.)

Abstract: The hydrogeochemical characteristics of groundwater are an important element in the study of the spatial and temporal variation of groundwater resources, which is crucial to water resources utilization, ecological environmental protection, and human development. Water samples were collected at eight observation of Nandong Karst Water System (NKWS) sites in each month of 2019, and the main ions and isotopes of the water samples were examined. The hydrogeochemistry characteristics of groundwater and its differences with surface water were explored by using the methods of multivariate statistics, Gibbs model. Results showed that the water chemistry types of groundwater were mainly HCO_3–Ca and HCO_3–Ca·Mg. The analysis of hydrogen and oxygen isotope showed that the initial recharge source of surface water and groundwater were atmospheric precipitation, and the measured hydrogen and oxygen isotopes of surface water were heavier due to the strong evaporation effect. The natural and anthropogenic processes contributed to the chemical composition of surface water and groundwater in the study area. However, the main factor affecting the quality of surface water and groundwater was the input of anthropogenic contaminants. In terms of natural factors, the main chemical ions of surface water and groundwater were mainly controlled by water-rock action originating from weathering and hydrolysis of rocks and soils. Ca^{2+}, Mg^{2+}, and HCO_3^- mainly originated from natural dissolution of carbonate rocks. K^+, Na^+, SO_4^{2-}, and Cl^- were partly from atmospheric precipitation. For human activities, Na^+ and Cl^- were partly from domestic water for local residents. SO_4^{2-} in surface water mainly came from mining. NO_3^- in groundwater mainly came from chemical fertilizers, and NO_3^- in surface water were mainly from human waste and domestic sewage.

Keywords: karst; hydrogeochemistry; isotope; ionic characteristics; controlling factors

check for updates

Citation: Zhu, X.; Liu, L.; Lan, F.; Li, J.; Hou, S. Hydrogeochemistry Characteristics of Groundwater in the Nandong Karst Water System, China. *Atmosphere* **2022**, *13*, 604. https://doi.org/10.3390/atmos13040604

Academic Editors: María Fernández-Raga, Yang Yu and Julian Campo

Received: 20 March 2022
Accepted: 7 April 2022
Published: 9 April 2022

Publisher's Note: MDPI stays neutral with regard to jurisdictional claims in published maps and institutional affiliations.

Copyright: © 2022 by the authors. Licensee MDPI, Basel, Switzerland. This article is an open access article distributed under the terms and conditions of the Creative Commons Attribution (CC BY) license (https://creativecommons.org/licenses/by/4.0/).

1. Introduction

The global karst area accounts for approximately 15% of the total global land area, and approximately 25% of the world's population relies on karst groundwater as the primary source for drinking and irrigation [1]. China is the country with the largest karst area distribution in the world, with karst area accounting for approximately 1/3 of the national land area, mainly in the southwest of China. Surface water and groundwater in karst areas are important water sources for local industrial and agricultural production and residential life. In the past decades, increasing environmental pollution caused by human activities [2], intentionally or unintentionally, has largely damaged sensitive karst ecosystems in many areas of China [3]. Karst aquifers constituting the main potable water resource are of heightened significance due to the increasing water demands and depletion of water resources [4].

The strata in karst areas are mainly composed of carbonate rocks, which are prone to form connected dissolution pipes, buckets, drop holes, and shafts of different sizes due to the erosion of carbonate rocks by unsaturated water bodies [5]. The presence of large voids makes it easier for surface water to rapidly recharge groundwater [6,7], which makes the rock formations significantly less efficient in filtering contaminants from surface recharge water sources. The soil layer is easily washed by surface water due to the relatively slow rate of karst soil formation [8]. Accordingly, the surface soil layer in karst areas is thin and even lithified in some areas [9], resulting in poor filtration, poor pre−purification, and rapid infiltration [10]. The special significance of the vulnerability of karst aquifers to degradation makes it imperative to acquire adequate knowledge of the karst groundwater hydrology. At present, a comprehensive understanding of surface and groundwater interactions in karst environments is lacking, including the geochemical mixing of surface and groundwater and the different reactivity of water with different geochemical properties to the aquifer host rock. The quality of surface and groundwater is mainly influenced by three main processes: (1) natural processes, such as lithology, water flow rate, quality of recharge water, interaction of water with soil and rocks, and interaction with other types of aquifers; (2) anthropogenic activities [3,11], including agriculture, industry, urban development, and the increase of water resources development; and (3) atmospheric input [12].

The Nandong Karst Water System (NKWS) is located in the economic development zone of Ge−Kai−Meng along the Kunhe River and is also the central township of Yunnan Province where political planning focuses on development. The land use types of NKWS have changed in recent years with the economic development and population growth in Mengzi and the surrounding areas [6]. The number of urban areas and industrial and mining areas has significantly increased. The factors affecting the quality of water bodies have gradually transitioned from being dominated by natural processes to being influenced by natural and anthropogenic processes [1]. This work presents a comprehensive analysis of the hydrogeochemistry characteristics of surface water and groundwater in NKWS by the integrated approach of isotopic ($\delta^{18}O$–H_2O, $\delta^{2}H$–H_2O), multivariate statistical analysis, and hydrochemical parameters. The objectives of this study are to (1) reveal the main ionic characteristics and spatial and temporal distribution patterns of surface water and groundwater in the study area during the rainy and dry seasons; (2) investigate the controlling factors of surface water and groundwater hydrochemistry in NKWS. This study would further the understanding and management of the karst aquifers, provide a basis for the rational exploitation and effective protection of surface water and groundwater in the karst area.

2. Study Area

The Nandong Underground River Basin is located in Honghe Prefecture of Yunnan Province and belongs to the suburbs of Gejiu and Kaiyuan cities and Mengzi City in the administrative division, with a basin area of 1684 km^2. It is a typical mega underground river basin in southwest China. The surface water mainly enters the Jijie Basin through the Hechongzha in the northwest and then flows out of the basin with the confluence of Zhadian River. Groundwater in the basin maintains relative independence, and karst water circulates in relatively independent units, constituting a series of karst water systems of varying sizes. Previously, the Nandong Underground River Basin was divided into the NKWS, the Datun−Jijie Karst Water System, and the karst water system in the southern part of Mengzi City. In this study, the NKWS in the basin was selected as the study area (Figure 1).

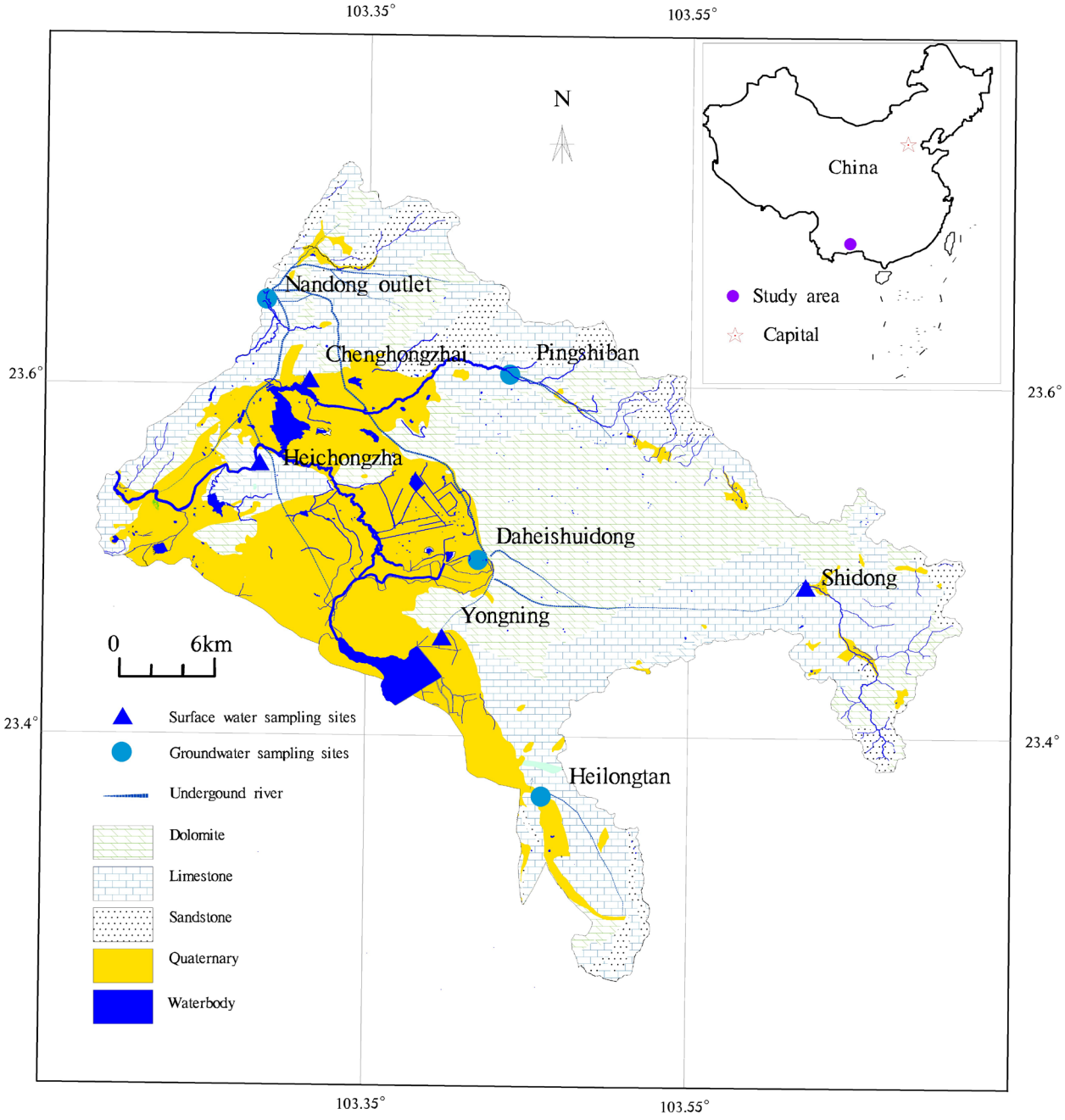

Figure 1. The hydrogeological map of NKWS. (created by the author).

2.1. Geological and Hydrogeological Setting

The sedimentary rocks in the Nandong underground river basin are widely distributed from the Paleozoic to the Quaternary, and the Upper Cambrian, Ordovician, Silurian, Jurassic and Cretaceous strata are missing, while the Lower and Middle Cambrian, Devonian, Carboniferous, Permian, Triassic, Tertiary and Quaternary are exposed, with a total thickness of 11,176 m. Among them, the Triassic strata are the most widely distributed, accounting for about 2/3 of the area of the region, while the Tertiary and Quaternary strata are mainly distributed in the basin areas, accounting for about 28% of the area of the region. The Paleozoic strata are concentrated in the area east of Mengzi and Daheishan. Basalt and granite are only found in the east of Dazhuang and near Youyi Village. The stratigraphy of this area is mainly pre-Cenozoic strata, and the structure is dominated by carbonate rocks,

and the exposed area of tuff and dolomite is about 1000 km^2. The subsidence basin area is mainly Cenozoic loose rocks, with a distribution area of about 450 km^2.

The NKWS is a karst water system with its boundary relatively closed and independent, whose boundary is composed of surface water divide, groundwater divide, water isolation or relative water isolation rock layer, and water barrier fault, covering an area of 1081.9 km^2. The thickness of karst aquifer reaches more than 1000 m, whose main aquifer is the carbonate rocks of the Triassic Gejiu Formation. The fracture structure in the system is developed, and the groundwater is runoff in the direction of the Nandong outlet. The NKWS consists of several parts: karst plateau, fractured basin, and inter−basin mound ridge. The NKWS has an early history of formation and complex runoff pathways, and is an underground river system formed by the superposition and combination of several underground rivers. It is divided into four subsystems according to the combination of each underground river and the relationship of supplemental runoff, namely, the No. 1 dark river subsystem of Nandong, the No. 2 and No. 3 dark river subsystems of Nandong, the Pingshiban dark river subsystem, and the Heilongtan dark river subsystem. The carbonate rocks in the system cover an area of 600 km^2 and produce approximately 560,000 m^3 water per square kilometer, with an average annual discharge of 357.8 million m^3. The depth of groundwater table is mostly below 100 m, and the variation of water level is 60–120 m.

2.2. Rainfall

The NKWS is on the Tropic of Cancer, with an average annual temperature of 17–18 °C, a mild climate, and distinct dry and wet seasons. Its annual rainfall is approximately 1200 mm. The annual rainfall in the flat area is 800 mm, while the plateau mountainous area is dry with little rainfall. The rainfall in the study area is mainly concentrated in May to October, with the most concentrated rainfall in July to August. It is dry with little rain from November to April of the following year. Rainfall is the main source of direct recharge of karst water in the area. According to statistics, 58% of the annual rainfall infiltrates and recharges to karst water, and 80–85% of the discharge of the underground river in Nandong area comes from rainfall. There is uneven distribution of rainfall in spatial and temporal scales, and the rainfall recharge received by water bodies in different areas is not consistent. The area around the top of Daheishan has the most abundant recharge, with annual rainfall of 1400–1500 mm. The seasonal outfalls in the area are mostly in the rainy season from June to September. The water volume in the Nandong basin exponentially increases from June to July, which reflects the seasonal changes in the strength of rainfall recharge. The karst mountainous area has exposed bedrock and developed superficial karst zone, with a few and thin soil distributed. The rainfall rapidly transforms from surface water to underground runoff, recharging karst water on a surface basis. In this work, we take May to October as the rainy season and January to April and November to December as the dry season. The water samples are classified as surface water in the rainy season (hereafter referred to as SR), surface water in the dry season (hereafter referred to as SD), groundwater in the rainy season (hereafter referred to as GR), and groundwater in the dry season (hereafter referred to as GD), according to the type and time of the water body.

3. Methods

3.1. Sampling and Analytical Procedures

Eight observation sites (four surface water and four groundwater sites) were evenly selected from upstream to downstream in the study area to comprehensively analyze the hydrogeochemical characteristics of the NKWS and its formation mechanism based on the previous results and meteorological data of the NKWS. Water samples were collected monthly from January to December 2019 at eight selected observation sites in the study area (from west to east: Shidong, Heilongtan, Pingshiban, Daheishuidong, Yongning, Chenghongzhai, Hechongzha, and the Nandong outlet). Heilongtan, Pingshiban, Daheishuidong, and Nandong outlet are groundwater observation points, while Shidong, Yongning, Chenghongzhai, and Heichongzha are surface water observation points (Figure 1).

Daheishuidong is the most important seasonal overflow cave in the east mountain of Caoaba, and it is located at the foot of the slope at the southeast edge of Caoaba Basin, 1.5 km from Caoaba Town. Only one water sample was taken in Daheishuidong because water flowed out only in January when sampling was done, while water samples were taken from the other seven sampling sites every month. There are 85 water samples in total. After each sampling, the water samples were sent to the laboratory for analysis of conventional components (mainly K^+, Na^+, Mg^{2+}, Ca^{2+}, HCO_3^-, SO_4^{2-}, NO_3^-, and Cl^-, etc.). Hydrogen and oxygen isotopes (D and ^{18}O) samples were sampled and tested since February. Surface water and groundwater samples were collected using 500 mL polyethylene sampling bottles. The bottles were washed three times with the original sample water before sampling. The original sample water was filtered with a 0.45 μm filter membrane. The filtered water samples were divided into two 500 mL sampling bottles and one 350 mL sampling bottle, with one 500 mL water bottle used for routine water chemistry component testing and the other 500 mL water bottle added with 1:1 nitric acid 2 mL to stabilize the metal elements in the water body, and 350 mL water samples are used for isotope detection.

All water samples were sealed and packed into a 4 °C shaded holding tank and transported to the laboratory as soon as possible to complete the tests. The water sample testing was undertaken by the Karst Geology and Resource Environment Testing Center of the Ministry of Natural Resources. The chemical reagents involved in the whole testing process were of analytical purity level. Blank control samples were set throughout the testing process. The quality assurance and control were achieved through the use of national level standards. The standard deviations of all the results of the water samples were less than 5%.

3.2. Pollution Evaluation

Single water quality evaluation method, also known as the single factor index method, belongs to the national standard method. This mechanism is the evaluation method used in the Environmental Quality Standard for Surface Water (GB3838−2002), and it is a widely used water quality evaluation method at present. Its essence is to simplify the analysis using actual measurement data and standard for comparison and classification and select the worst water quality category as the evaluation results. In this study, the water quality single factor index method was used to evaluate the pollution of the main anions and cations in the surface water (pH, Cl^-, SO_4^{2-}, NO_3^-, NH_4^+, and COD) and groundwater (pH, Na^+, Cl^-, SO_4^{2-}, NO_3^-, NO_2^-, NH_4^+, TDS, and COD) of NKWS, calculated as Equation (1) [13], as follow:

$$Pi = Ci/Si \quad (1)$$

where *Pi* is the single factor index, *Ci* is the measured concentration of the evaluation factor, and *Si* is the evaluation standard concentration of the evaluation factor, the unit of both is mg/L. In the single index of surface water, the standard concentration in the III water quality standard of Environmental Quality Standard for Surface Water (GB3838−2002) was selected as *Si*. In the single index of groundwater, the standard concentration in the III water quality standard of Standard for Groundwater Quality (GB/T14848−2017) was selected as *Si*. The single pollution index of each factor of the water sample was obtained according to Equation (1).

4. Results

4.1. Water Chemical Characteristics of Groundwater

The statistical results of the main indicators of water chemistry of groundwater and surface water in the study area are shown in Tables 1 and 2, and the statistical characteristics of each ion are shown in Figure 2. The change of each major ion concentration was mainly influenced by the ion characteristics, the solubility of the compounds which was composed of ions, and its hydrogeochemical environment. The pH values of Groundwater ranged from 7.15 to 7.59, with an average value of 7.38, which was weakly alkaline. TDS in the groundwater and surface water varied from 229.22 mg/L to 437.23 mg/L, and its average

value of groundwater was 317.19 mg/L, which was slightly greater than the average value of surface water (315.76), indicating that the groundwater and surface water were low mineralization water and fresh water, respectively. The overall water quality was relatively good.

Table 1. Statistics of water chemistry parameters in groundwater (N = 37).

		pH	Concentration (mg/L)												
			K^+	Na^+	Ca^{2+}	Mg^{2+}	Cl^-	SO_4^{2-}	HCO_3^-	NO_3^-	NO_2^-	NH_4^+	TDS	COD_{Mn}	Hardness
Rain season	Min	7.15	0.57	0.76	68.71	13.78	1.18	11.68	221.92	2.68	nd	nd	229.22	nd	187.92
	Max	7.59	4.71	45.10	96.00	20.98	25.34	90.94	312.28	20.87	0.690	0.60	437.23	0.97	318.79
	Mean	7.38	1.61	9.57	83.84	15.82	7.61	43.76	279.42	10.77	0.084	0.05	317.19	0.35	270.33
	SD	0.12	1.18	12.81	7.48	2.20	6.02	25.10	27.04	4.51	0.184	0.13	48.01	0.20	32.20
	CV%	1.68	73.71	133.83	8.93	13.89	79.16	57.36	9.68	41.92	219.88	269.16	15.14	58.09	11.91
	Exceedance/%	0	-	0	-	-	0	0	-	0	0	0	0	0	0
Dry season	Min	7.20	0.78	1.10	79.52	12.49	1.19	7.58	247.40	5.58	nd	nd	271.92	nd	254.23
	Max	7.96	3.70	33.87	95.59	22.10	18.69	79.36	318.78	15.78	2.660	0.09	388.64	1.64	329.25
	Mean	7.44	1.56	7.87	86.28	16.53	6.49	38.34	295.41	10.70	0.179	0.02	322.97	0.45	283.55
	SD	0.17	0.93	9.88	5.53	2.76	4.82	22.62	16.63	2.57	0.593	0.02	34.59	0.40	23.70
	CV%	2.25	59.62	125.46	6.41	16.72	74.30	58.99	5.63	24.03	332.09	104.59	10.71	88.16	8.36
	Exceedance/%	0	-	0	-	-	0	0	-	0	0	0	0	0	0
All	Min	7.15	0.57	0.76	68.71	12.49	1.18	7.58	221.92	2.68	nd	nd	229.22	nd	187.92
	Max	7.96	4.71	45.10	96.00	22.10	25.34	90.94	318.78	20.87	2.660	0.60	437.23	1.64	329.25
	Mean	7.41	1.58	8.70	85.09	16.18	7.04	40.98	287.63	10.73	0.132	0.03	320.16	0.40	277.12
	SD	0.15	1.06	11.43	6.67	2.53	5.47	24.01	23.70	3.65	0.446	0.10	41.76	0.32	28.92
	CV%	2.04	67.10	131.40	7.83	15.63	77.74	58.60	8.24	33.99	337.06	284.69	13.04	80.11	10.44
	Exceedance/%	0	-	0	-	-	0	0	-	0	0	0	0	0	0
Standard value		6.5–8.5	-	200	-	-	250	250	-	88.57	3.29	0.64	1000	3.0	450

nd means not detected, "-" means no reference value and corresponding calculated value.

Table 2. Statistics of water chemistry parameters in surface water (N = 48).

		pH	Concentration (mg/L)												
			K^+	Na^+	Ca^{2+}	Mg^{2+}	Cl^-	SO_4^{2-}	HCO_3^-	NO_3^-	NO_2^-	NH_4^+	TDS	COD_{Mn}	Hardness
Rain season	Min	6.84	2.50	1.81	36.98	11.87	4.16	4.54	77.62	nd	nd	nd	166.97	1.27	146.68
	Max	7.44	10.71	23.92	115.70	25.32	39.46	156.61	267.78	42.060	1.240	2.66	476.14	5.17	393.20
	Mean	7.23	5.44	12.21	66.79	18.02	23.77	95.83	162.08	3.801	0.097	0.34	313.11	2.65	240.56
	SD	0.15	2.30	6.35	23.51	4.15	11.05	51.39	52.65	8.527	0.282	0.63	92.94	1.01	71.97
	CV%	2.04	42.21	52.01	35.21	23.02	46.50	53.63	32.49	224.34	291.91	186.78	29.68	38.34	29.92
	Exceedance/%	0	-	-	-	-	0		-	0	-	4.17	-	0	-
Dry season	Min	7.24	1.56	1.06	26.43	12.68	2.19	3.26	77.62	nd	nd	nd	127.72	0.59	118.26
	Max	7.78	11.64	23.65	102.70	26.56	38.37	147.38	266.74	42.430	1.540	7.46	447.38	5.26	355.67
	Mean	7.46	5.77	12.14	63.47	19.32	20.99	85.33	176.15	6.141	0.261	0.75	310.28	2.44	241.36
	SD	0.12	2.51	6.07	23.31	2.96	10.40	52.79	48.60	10.474	0.449	1.57	90.89	1.01	66.88
	CV%	1.66	43.47	50.02	36.73	15.32	49.53	61.87	27.59	170.56	171.65	209.01	29.29	41.53	27.71
	Exceedance/%	0	-	-	-	-	0		-	0	-	16.67	-	0	-
All	Min	6.84	1.56	1.06	26.43	11.87	2.19	3.26	77.62	nd	nd	nd	127.72	0.59	118.26
	Max	7.78	11.64	23.92	120.72	26.56	39.46	159.40	267.78	42.430	4.460	7.46	505.24	5.26	406.92
	Mean	7.34	5.55	12.16	66.32	18.80	22.51	92.12	170.86	5.173	0.266	0.53	315.76	2.55	244.41
	SD	0.18	2.41	6.15	24.55	3.77	10.74	52.72	52.30	9.627	0.719	1.19	95.10	1.01	72.77
	CV%	2.40	43.32	50.59	37.01	20.04	47.69	57.23	30.61	186.10	269.85	225.80	30.12	39.58	29.77
	Exceedance/%	0	-	-	-	-	0	0	-	0	-	10.42	-	0	-
Standard value		6–9	-	-	-	-	250	250	-	44.29	-	1.29	-	20	-

nd means not detected, "-" means no reference value and corresponding calculated value.

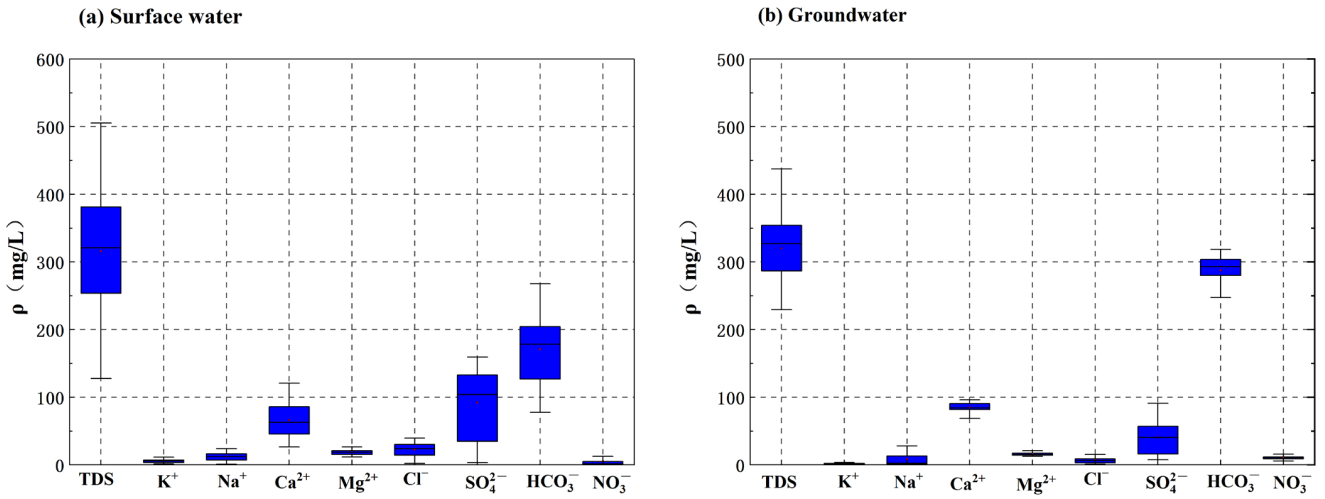

Figure 2. Statistical characteristics of surface water (**a**) and groundwater (**b**) major ions in NKWS.

According to the classification standard of hardness range (mg/L number of $CaCO_3$): water whose total hardness is less than 75 mg/L is very soft water; 75–150 mg/L is soft water; and 150–300 mg/L is slightly hard water. Table 1 illustrates that groundwater in the study area were mainly slightly hard water. The average values of HCO_3^- and Ca^{2+} concentrations in Groundwater were the largest among all of anions and cations, respectively, and their coefficient of variation was small. The result indicated that the absolute contents of HCO_3^- and Ca^{2+} in the water in the study area were the highest, with its spatial variability relatively small and distribution relatively stable. Ca^{2+} was the most dominant cation, with mass concentrations in the groundwater and surface water ranging from 68.71 mg/L to 96.00 mg/L, averaging 85.09 mg/L, accounting for 76.28% of the measured mass concentrations of the major cations (Ca^{2+}, Mg^{2+}, Na^+, and K^+) in groundwater. Mg^{2+} was the second major cation, with a concentration in the groundwater and surface water range of 12.49 mg/L to 22.10 mg/L, averaging 16.18 mg/L. HCO_3^- was the most dominant anion, with a mass concentration in groundwater of 221.92–318.78 mg/L, averaging 221.69 mg/L, accounting for 83.04% of the measured mass concentrations of the main anions (HCO_3^-, SO_4^{2-}, Cl^-, and NO_3^-) in groundwater. SO_4^{2-} was the next major anion, with concentrations in groundwater ranging from 7.58 mg/L to 90.94 mg/L and an average of 40.98 mg/L. SO_4^{2-} in surface water was much larger than that in groundwater, which mainly originated from the dissolution of evaporites (mainly sulfate rocks), oxidation of sulfides, and human activities, such as fossil fuel combustion. COD is one of the important indicators reflecting water quality. COD_{Mn} in groundwater samples from the NKWS ranged from nd (meant not detected) to 1.64 mg/L, with a mean value of 0.4 mg/L, which was lower than 3.0 mg/L (III water quality's COD_{Mn} standard of Standard for Groundwater Quality (GB/T14848−2017)). COD_{Mn} in surface water ranged from 0.59 mg/L to 5.26 mg/L, with a mean value of 2.55 mg/L, which was lower than 20.0 mg/L (III water quality's COD standard of Environmental Quality Standard for Surface Water (GB3838−2002)), indicating that the surface water quality in the study area was generally good, but some sample sites COD_{Mn} were higher than 3.0 mg/L (water quality's COD_{Mn} standard of Standards for Drinking Water Quality), especially in the rainy season, reflecting that surface water was more influenced by human activities, and the water quality in the surface water was worse than that in the groundwater. COD_{Mn} in surface water ranged from 0.59 mg/L to 5.26 mg/L, with a mean value of 2.55 mg/L, which was lower than 20.0 mg/L (III water quality's COD standard of Environmental Quality Standard for Surface Water (GB3838−2002)), indicating that the surface water quality in the study area was generally good, but some sample sites COD_{Mn} were higher than 3.0 mg/L (water quality's COD_{Mn} standard of Standards for Drinking Water Quality), especially in the rainy season, reflecting that surface water was more influenced by human activities, and the water quality in the surface water was worse than that in the groundwater.

The order of major cation content in groundwater in the study area was: $Ca^{2+} > Mg^{2+} > Na^+ > K^+ > NH_4^+$. The order of major anion content in groundwater was: $HCO_3^- > SO_4^{2-} > NO_3^- > Cl^- > NO_2^-$. According to the III water quality standard of the Standard for Groundwater Quality (GB/T14848−2017), there were no ions in groundwater exceeding the standard. According to the III water quality standard of the Environmental Quality Standard for Surface Water (GB3838−2002), only NH_4^+ in surface water exceeds the standard value of 1.29 mg/L, and its exceedance rate was 10.42%. The exceedance rate of surface water in the rainy season was 4.17%, with its maximum concentration being 2.66 mg/L, and the exceedance multiple was 2.06 times. The exceedance rate of surface water in the dry season was 16.67%, with its maximum concentration being 7.46 mg/L, and the exceedance multiple was 5.78 times. The exceedance of NH_4^+ was higher in the dry season than that in the rainy season.

The concentrations of Ca^{2+} and HCO_3^- in groundwater were significantly higher than those in surface water because groundwater reacted with major minerals in aquifer rocks (limestone, dolomite, marl, etc.) during runoff in karst areas, dissolving or precipitating some water chemical components. Accordingly, Ca^{2+} and HCO_3^- are enriched. However,

surface water flowed fast, quickly renewed, and had weak water-rock interactions. The large coefficients of variation of NO_3^-, NO_2^-, and NH_4^+ in surface water and Na^+, NO_2^-, and NH_4^+ in groundwater regardless of the rainy or dry seasons, indicated that their spatial variability was large and easily influenced by external factors. Na^+ concentration in the groundwater and surface water ranged from 0.76 mg/L to 45.10 mg/L, with an average of 10.56 mg/L. Its coefficient of variation in the groundwater reached 131.40%, which was mainly related to the geological environment. The NO_3^- concentration in the groundwater and surface water ranged from 0.05 mg/L to 42.43 mg/L, with an average of 9.77 mg/L. Its coefficient of variation in the surface water reached 186.56%, which was mainly influenced by human activities.

4.2. Water Chemistry Type

The water chemistry characteristics of water bodies in the region can be objectively reflected by drawing a Piper diagram. In this work, water chemistry types were classified according to Shukarev classification [14]. The position of the test results for 85 water samples of the NKWS in the Piper diagram is shown in Figure 3. According to the partitioning of the Piper diagram, the samples falling in different areas of the rhombus have different water chemistry properties. Most water samples fell in areas where carbonic acid hardness exceeds 50%, and water chemistry was dominated by alkaline earth metals and weak acids. Only a few sampling sites in Yongning and Hechongzha fell in areas with non-carbonate hardness above 50% and none with anion and cation pairs above 50%.

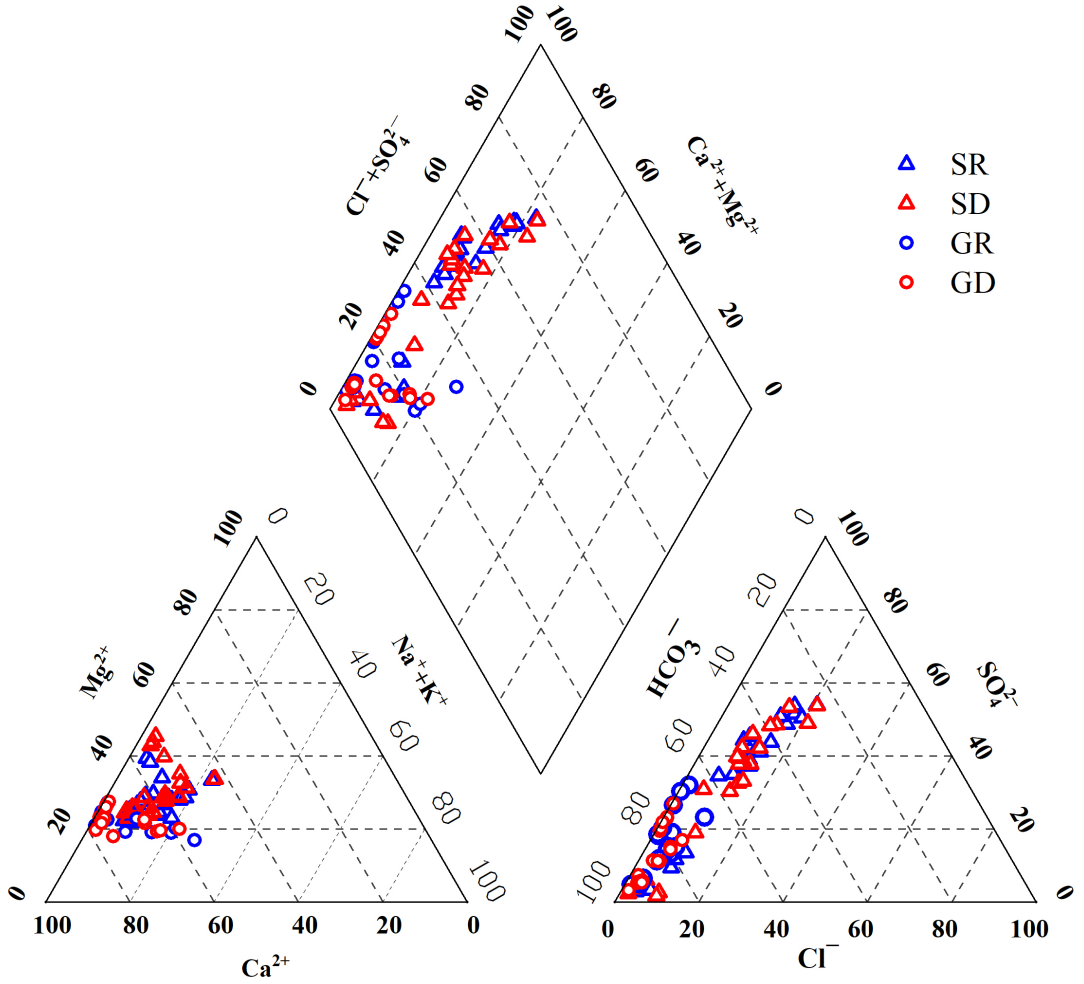

Figure 3. Piper diagram of water samples in NKWS.

The anions of the surface water and groundwater samples were all located in the lower left corner of the anion triangle diagram, and HCO_3^- was the dominant ion with an average equivalent concentration of 67.19% of all anions, indicating that carbonate rock weathering is the main source of aqueous proton, followed by SO_4^{2-} with an average of 24.93% of all anions. The cations of the surface water and groundwater samples were located in the lower left corner of the cation triangle diagram, with the dominant cation being Ca^{2+}, accounting for 64.03% of all cations, followed by Mg^{2+}, accounting for 26.33% of all cations. The ionic composition of the surface water and groundwater showed high consistency. Groundwater was more concentrated in the lower left corner of the ion triangle map compared with surface water due to the long-term experience of water-rock interaction. With the control of carbonate strata in the karst area, the water chemistry types of the surface water in the study area were $HCO_3 \cdot SO_4$–Ca·Mg (47.92%), HCO_3–Ca·Mg (27.08%), and $HCO_3 \cdot SO_4$–Ca (25.00%), and the water chemistry types of the groundwater were mainly HCO_3–Ca (75.68%) and HCO_3–Ca·Mg (19.22%). From the perspective of individual analysis of each observation, the water chemistry type of Yongning, Hechongzha, and Chenghongzhai in surface water was mainly $HCO_3 \cdot SO_4$–Ca·Mg type, while Shidong was HCO_3–Ca·Mg type water. In groundwater, the water chemistry type of Heilongtan and Nandong was HCO_3–Ca type, while Ping Shiban was mainly HCO_3–Ca·Mg type water. The above results showed that the surface water and groundwater were affected by the weathering dissolution of carbonate rocks.

5. Discussion

5.1. Correlation between Different Ions

The correlation of water chemical components can reflect the consistency and difference between ionic components and reveal the material source of ions or the chemical reaction process that they undergo. The correlation of ions with the same material source or undergoing the same chemical reaction process is generally better. The Pearson correlation coefficient matrix is more frequently used to quantify the correlation of the components in hydrogeochemical studies. The Pearson correlation coefficient matrixes for surface water and groundwater chemical parameters in the study area are shown in Table 3. In surface water, K^+, Na^+, and Cl^- showed a significant positive correlation with each other. Ca^{2+}, Mg^{2+}, and SO_4^{2-} showed a highly significant positive correlation with each other. Ca^{2+} and HCO_3^- showed a highly significant positive correlation with each other. In groundwater, K^+, Na^+, and Cl^- showed a highly significant positive correlation with each other. Ca^{2+}, Mg^{2+}, and SO_4^{2-} showed a highly significant positive correlation. Ca^{2+} and Mg^{2+} showed a highly significant positive correlation. This result reflected the sequence of dissolving rock components in water: chlorate was an easily soluble component, which meant that K^+, Na^+, and Cl^- were dissolved into groundwater at the earliest, followed by sulfate, indicating that Ca^{2+}, Mg^{2+}, and SO_4^{2-} were more difficult to be dissolved into groundwater, and the insoluble carbonate (Ca^{2+} and HCO_3^-) were finally transferred into the groundwater.

5.2. Multivariate Statistical Analysis

According to the principal component analysis of the major ions in surface water (Table 4, Figure 4), the cumulative variance of the first two components accounted for 71.33% of the total variance. The contribution of the first component was 47.11%, which was more correlated with K^+, Mg^{2+}, Cl^-, SO_4^{2-}, and NO_3^-. The contribution of the second component accounted for 24.23%, which was more correlated with Na^+, Ca^{2+}, and HCO_3^-. According to the principal component analysis of the major groundwater ions (Table 4, Figure 4), the cumulative variance of the first two components accounted for 68.546% of the total variance. The first component accounted for 39.96% and was more correlated with K^+, Na^+, Cl^-, and HCO_3^-; the second component accounted for 28.58% and was more correlated with Ca^{2+}, Mg^{2+}, SO_4^{2-}, and NO_3^-.

Table 3. Correlation coefficient matrix of water chemistry parameters in NKWS.

		Na^+	K^+	Ca^{2+}	Mg^{2+}	HCO_3^-	Cl^-	SO_4^{2-}	NO_3^-	NO_2^-	NH_4^+	TDS	COD_{Mn}	pH
Surface water	Na^+	1.000												
	K^+	0.353 *	1.000											
	Ca^{2+}	0.246	−0.089	1.000										
	Mg^{2+}	0.463 **	−0.042	0.737 **	1.000									
	HCO_3^-	−0.472 **	−0.140	0.518 **	0.356 *	1.000								
	Cl^-	0.889 **	0.333 **	0.537 **	0.609 **	−0.257	1.000							
	SO_4^{2-}	0.748 *	0.058	0721 **	0.666 **	−0.178	0.867 **	1.000						
	NO_3^-	0.203	0.137	0.301 *	0.236	−0.040	0.234	0.265	1.000					
	NO_2^-	0.095	−0.143	0.371 **	0.356 *	0.160	0.160	0.309 *	0.301 *	1.000				
	NH_4^+	0.131	0.567 **	0.036	−0.052	−0.047	0.204	0.131	−0.143	−0.096	1.000			
	TDS	0.556 **	0.091	0.931 **	0.820 **	0.282	0.768 **	0.876 **	0.354 *	0.378 **	0.108	1.000		
	COD	0.437 **	0.609 **	0.155	0.173	−0.153	0.513 **	0.364 *	−0.014	0.137	0.318 *	0.556 **	1.000	
	pH	0.150	0.244	0.165	0.218	0.160	0.139	0.140	0.260	0.201	0.292 *	0.242	0.142	1.000
groundwater	Na^+	1.000												
	K^+	0.921 **	1.000											
	Ca^{2+}	−0.133	−0.189	1.000										
	Mg^{2+}	−0.130	−0.201	0.682 **	1.000									
	HCO_3^-	0.400 *	0.345 *	0.300	0.049	1.000								
	Cl^-	0.944 **	0.876 **	−0.233	−0.292	0.471 **	1.000							
	SO_4^{2-}	0.188	0.151	0.524 **	0.698	−0.320	−0.127	1.000						
	NO_3^-	0.182	0.179	0.360 *	−0.149	−0.045	0.116	0.231	1.000					
	NO_2^-	0.110	0.065	−0.117	0.052	0.014	0.074	−0.056	−0.282	1.000				
	NH_4^+	.0.024	0.247	−0.384 *	−0.155	−0.157	−0.018	−0.099	−0.343 *	−0.036	1.000			
	TDS	0.661 **	0.586 **	0.556 **	0.517 **	0.321	0.499 **	0.719 **	0.322	−0.003	−0.182	1.000		
	COD	0.092	0.175	−0.185	−0.115	0.002	0.104	−0.133	−0.180	0.588 **	0.283	−0.054	1.000	
	pH	−0.208	−0.127	0.274	0.453 **	0.020	−0.230	0.233	−0.088	−0.307	0.170	0.107	−0.114	1.000

* Significant at 0.01 level. ** Significant at 0.05 level.

Table 4. PCA representation for surface water samples and groundwater samples in Nandong Karst Water System (NKWS).

Variables	Surface Water		Groundwater	
	PC1	PC2	PC1	PC2
Na^+	0.115	−0.346	0.516	0.134
K^+	0.421	−0.354	0.524	0.178
Ca^{2+}	0.376	0.447	−0.167	0.546
Mg^{2+}	0.403	0.320	−0.224	0.518
Cl^-	0.482	−0.178	0.542	0.056
SO_4^{2-}	0.483	−0.013	−0.067	0.559
HCO_3^-	−0.034	0.648	0.273	0.112
NO_3^-	0.199	0.023	0.089	0.238
Initial Eigen values	3.767	1.938	3.197	2.287
% of variance	47.106	24.227	39.962	28.584
Cumulative % of Variance	47.106	71.334	39.962	68.546

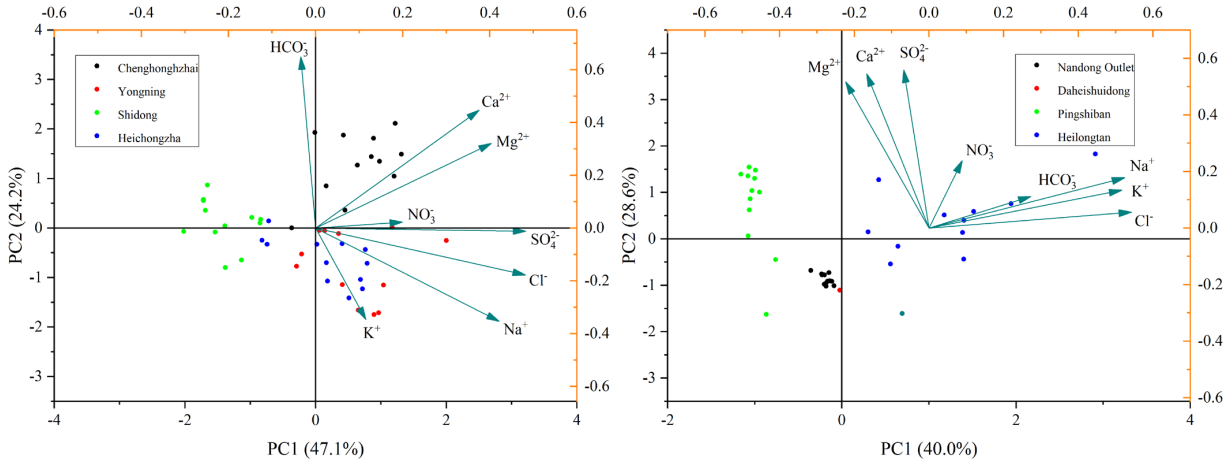

Figure 4. PCA representation for surface water samples and groundwater samples.

The variables for the factor analysis in this study were Ca^{2+}, Mg^{2+}, Na^{+}, K^{+}, HCO_3^{-}, SO_4^{2-}, Cl^{-}, and NO_3^{-}. The potential sources of NO_3^{-} contamination in the study area included chemical fertilizer (urea, ammonium sulfate, and N/P/K fertilizer mix) applied in the cultivated land, soil organic matter, effluent derived from the septic system, livestock waste, and atmospheric deposition. No primary contamination of NO_3^{-} was found, and atmospheric deposition was not considered to be a major source of the NO_3^{-} concentrations in the surface water and groundwater. Accordingly, the substantial contribution of NO_3^{-} in the study area was likely resulted from the excessive application of agricultural fertilizers and sewage effluents. Na^{+} in surface water and groundwater derived from the incongruent dissolution of plagioclase in granite, chemical fertilizer, domestic effluents, and atmospheric input [15–18]. K^{+} in surface water and groundwater often comes from orthoclase and muscovite minerals present in granite, chemical fertilizer and domestic effluents. The potential sources for Cl^{-} included natural sources (dissolution of minerals), atmospheric deposition [19], agricultural chemicals (potash or KCl), animal waste, and septic effluent [17,18,20–22]. Given that there was little significant material source for Cl^{-} in the surface water and groundwater in the Triassic carbonates (limestone and dolomite) and sediments since Quaternary, Cl^{-} in the surface water and groundwater could only originate from rainfall recharge and human activities in the study area. Sources of SO_4^{2-} included rainfall, fertilizers [17,18,23], sewage effluents, and dissolution of sulfide minerals present in granite. However, it was underlain by limestone and dolomite rather than by granite in the study area. The outcrops in the study area were mainly carbonate rocks (limestone and dolomite) of Triassic age and Quaternary deposits, with a minor amount of sandstone (Figure 1). Ca^{2+} and HCO_3^{-} in surface water and groundwater primarily came from the dissolution of carbonate in karst area. Mg^{2+} in groundwater often came from the input of the dissolution of dolomite in karst areas [15,16,23].

In the surface water and groundwater, Factor 1 can be reasonably assumed to be indicative of the contamination sources related to human activities. Meanwhile, Factor 2 can be assumed to be indicative of water-rock interaction. HCO_3^{-} exhibited a high loading in Factor 2 (0.273), indicating that anthropogenic CO_2 gas supplies HCO_3^{-} to the groundwater and should be regarded as a potential source of HCO_3^{-} in the groundwater near the residential areas. Lastly, NO_3^{-} showed high loading in Factor 2 (0.238) in the groundwater, suggesting that soil organic matters are an important source for NO_3^{-} in the groundwater. In surface water, the samples of Shidong had a high score on PC1, indicating that its water chemistry was mainly influenced by human activities. The reason is that there were large areas of farmland around the site, and the fertilizer applied in the agricultural farming process had a greater impact on the water quality of this area. The samples of other points were more evenly distributed on PC1 and PC2, indicating that they were affected by human activities and water-rock interaction. The Pingshiban and Heiongtan groundwater samples had higher scores on PC1, indicating that their water chemistry was mainly influenced by human activities due to the large areas of farmland nearby, and the fertilizer applied in the agricultural cultivation process had a great impact on water chemistry. The higher score of Nandong Outlet on PC2 indicated that its water chemistry was mainly influenced by water-rock interaction.

In summary, the results suggested that natural and anthropogenic processes may contribute to chemical composition of surface water and groundwater. However, the input of anthropogenic pollutants should be considered the major source that influences the surface water and groundwater quality in NKWS.

5.3. Natural Environmental Influences

5.3.1. Atmospheric Precipitation

There were evident seasonal variations of hydrogen and oxygen stable isotopes in precipitation in the study area, with a negative bias in the rainy season and a heavy bias in the dry season, as well as an obvious rainfall effect [24]. The Local Meteoric Water Line

(LMWL) equation (Equation (2)) was created on the basis of the precipitation isotope data from August 2014 to July 2015 as follows:

$$\delta D = 8.08\delta^{18}O + 8.38,\ R^2 = 0.9926 \quad (2)$$

Its slope is 8.08, which did not differ much from the Global Meteoric Water Line (GMWL) (Craig, 1961) (Equation (3)):

$$\delta D = 8\delta^{18}O + 10 \quad (3)$$

The intercept of GMWL was slightly smaller than the GMWL, which reflected that evaporation was strong in the region. The main cause was that the study area was in a highland region with a dry climate, and a significant part of the water vapor came from local evaporation and the heavy isotopes produced during the landing of raindrops under arid climatic conditions due to evaporation fractionation [25], resulting in high $\delta^{18}O$ in precipitation and causing deviations in slope and intercept.

Table 5 shows the statistics of hydrogen and oxygen isotope parameters of water samples. When the hydrogen and oxygen isotope values of all water samples were projected onto the δD–$\delta^{18}O$ relationship diagram (Figure 5), the hydrogen and oxygen isotope values of groundwater were more concentrated compared with surface water points and clustered and distributed near the LMWL. This result indicated that the initial recharge sources of surface water and groundwater were mainly atmospheric precipitation, and the evaporation of atmospheric precipitation was few during infiltration through soil and bedrock into the subsurface. The samples of surface water were mostly distributed in the lower right of the LMWL, indicating that their initial recharge sources were mainly atmospheric precipitation. The measured hydrogen and oxygen isotopes were heavy due to the strong evaporation effect.

Table 5. Statistical characteristics of hydrogen and oxygen isotopes.

	Surface Water				Groundwater				All			
	Min	Max	Mean	SD	Min	Max	Mean	SD	Min	Max	Mean	SD
δD (‰)	−80.60	−24.20	−52.64	13.49	−86.40	−69.70	−73.75	2.79	−86.40	−24.20	−61.68	14.71
$\delta^{18}O$ (‰)	−11.04	−2.07	−6.53	2.36	−10.42	−9.46	−10.14	0.19	−11.04	−2.07	−8.08	2.53

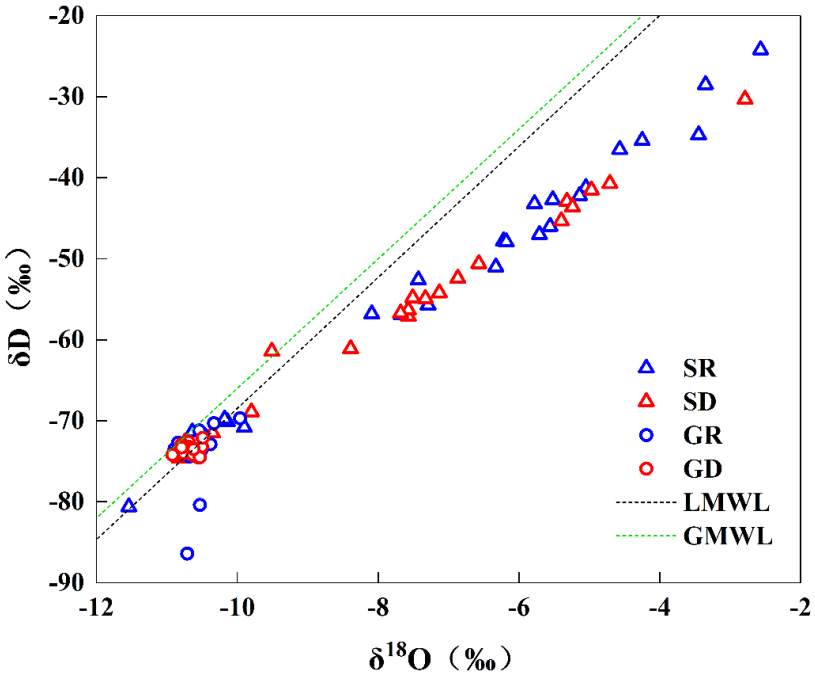

Figure 5. Distribution of δ^2H and $\delta^{18}O$ in NKWS.

5.3.2. Major Natural Mechanisms Controlling Water Chemistry

The Gibbs diagram is a qualitative study of the chemical composition and origin of natural waters. Gibbs and Feth [26,27] used the relationship diagrams of TDS $-$ $Na^+/(Na^+ + Ca^{2+})$ and TDS $-$ $Cl^-/(Cl^- + HCO_3^-)$ to classify natural waters into three main control types, namely, precipitation type, rock weathering dissolution filtration type, and evaporative concentration type. The water samples with low TDS and high cation concentration ratio ($Na^+/(Na^+ + Ca^{2+})$ close to 1) are mainly distributed in the lower right corner of the Gibbs diagram, indicating that the water samples mainly receive recharge from precipitation. Water samples with medium TDS and low cation concentration ratio ($Na^+/(Na^+ + Ca^{2+})$ generally less than or equal to 0.5) are mainly distributed in the left side of the middle of Gibbs diagram. This type of water samples' composition is controlled by the weathering and filtration of rocks, and the composition of such water points mainly comes from the weathering hydrolysis of rocks and soils. The water samples with high TDS and high cation concentration ratio ($Na^+/(Na^+ + Ca^{2+})$ close to 1) are distributed in the upper right corner of the Gibbs diagram, indicating that the water chemical composition of the water sample is controlled by the evaporative concentration. This type of water samples are generally distributed mainly in the arid areas where evaporation is strong. The same principle of analysis by anion concentration ratio ($Cl^-/(Cl^- + HCO_3^-)$) can be used to check each other by comparative analysis of anions and cations.

The water chemistry data of the samples in the study area were cast onto the Gibbs diagram to verify the above hydrogeochemical effects (Figure 6). The surface water and groundwater water samples in the wet and dry seasons were distributed in the left side of the middle of the Gibbs diagram, and the water samples had medium TDS and low ion concentration ratios. The $Na^+/(Na^+ + Ca^{2+})$ values of the surface water samples varied from 0.038 to 0.351, and its $Cl^-/(Cl^- + HCO_3^-)$ values ranged from 0.011 to 0.342. The values of $Na^+/(Na^+ + Ca^{2+})$ of the groundwater samples were in the range of 0.013 to 0.331, and its $Cl^-/(Cl^- + HCO_3^-)$ values ranged from 0.004 to 0.078. This result indicated that the chemical composition, migration transformation, and ion sources of groundwater in the study area during the rainy and dry seasons were highly consistent, and that water-rock action was the main controlling factor of groundwater chemical components. Hence, ions mainly originated from the weathering dissolution of rocks and soil, which was consistent with the fact that bodies were affected by rock weathering in the karst area water [28]. The main reason was the predominance of carbonate rocks in the stratum of NKWS. The longer the water acted with carbonate rocks, the faster the dissolution weathering rate of carbonate rocks was. The anion ratio diagram shows that the $Cl^-/(Cl^- + HCO_3^-)$ values of surface water were higher than those in groundwater, indicating that the Cl^- content in surface water was higher than that in groundwater, which mainly originated from the input of precipitation, domestic sewage, and agricultural farming activities [29].

5.3.3. Water-Rock Interactions

The Gibbs diagram demonstrates that the surface water and groundwater chemical components of NKWS were mainly controlled by water-rock interaction. The linear relationship between $SO_4^{2-} + Cl^-$ and HCO_3^- was used to further identify the controlling ratios of carbonate and evaporite rocks. The point located at the upper left side of the 1:1 relationship line is from carbonate karst, and the point located at the lower right side is from evaporite karst (gypsum and NaCl, etc.) [25]. As shown in Figure 7 shows that all 37 groundwater samples were distributed in the range of carbonate karst erosion. Half of the surface water samples fell into the range of carbonate karst erosion and half into the range of evaporite salt karst erosion. Considering that the sources of SO_4^{2-} and Cl^- in surface water included water-rock action, mineral mining, and agricultural farming, and combining with the distribution of mines and lithology in the study area, it was less likely that the surface water points are affected by rock types such as gypsum ($CaSO_4$-H_2O) and NaCl. Therefore, the content of SO_4^{2-} and Cl^- in surface water was mainly related to human activities around the sampling sites, including mineral mining, agricultural farming, and domestic sewage.

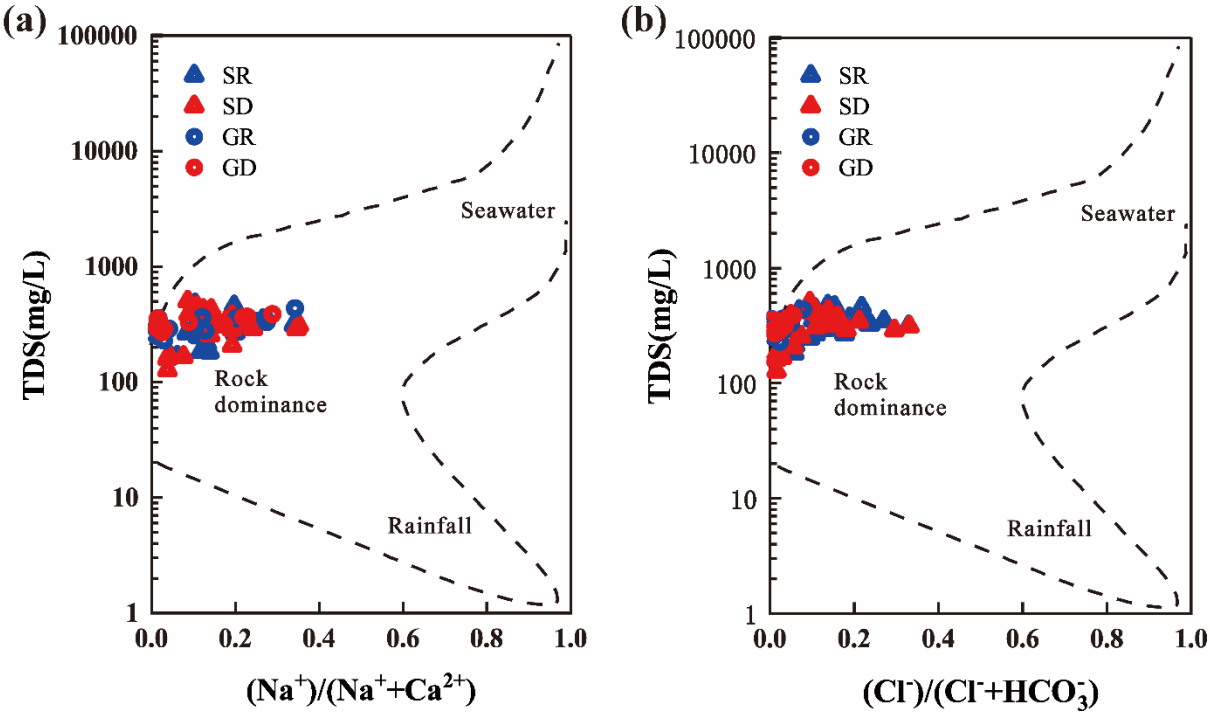

Figure 6. Identification of the main processes on Gibbs diagrams (adapted from Gibbs 1970) according to (**a**) the Na and Ca ratio (**left**) and (**b**) the Cl and HCO_3 ratio (**right**).

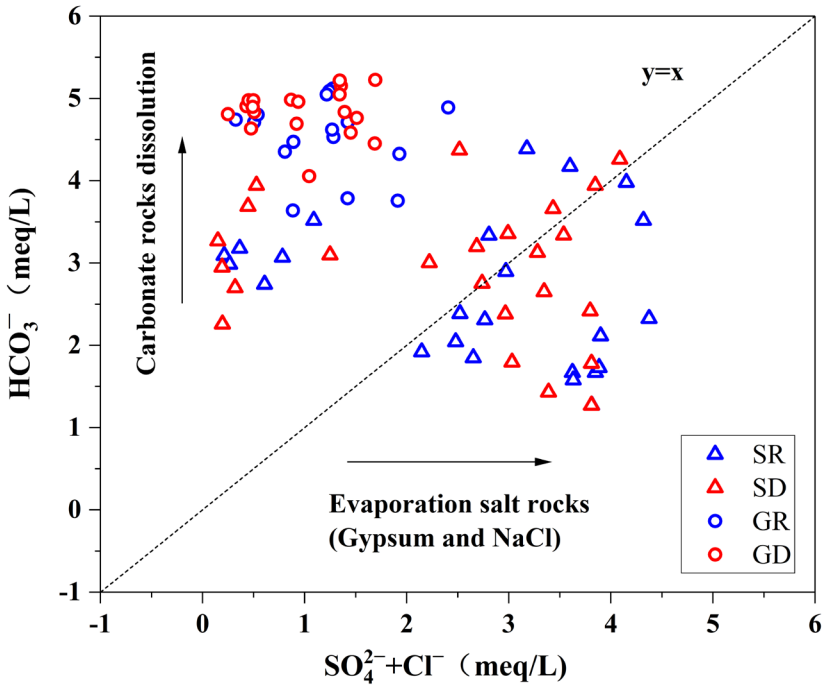

Figure 7. Relationship between (SO_4^{2-} + Cl^-) and HCO_3^-.

Groundwater in the study area was mainly controlled by carbonate rocks, which mainly include limestone and dolomite, consisting of calcite ($CaCO_3$) and dolomite ($CaMg(CO_3)_2$), respectively. Ca^{2+}, Mg^{2+}, and HCO_3^- mainly originated from the dissolution of rocks. Limestone dissolves to form Ca^{2+} and HCO_3^-, and dolomite dissolves to form Ca^{2+}, Mg^{2+}, and HCO_3^-, while the dissolution rate of limestone is higher than that of dolomite. The dissolution process of groundwater flowing through calcite and dolomite is shown in Equations (4) and (5). When pure calcite dissolution reaches equilibrium, the ratio of Mg^{2+} to Ca^{2+} in groundwater is 0.

When pure dolomite dissolution reaches equilibrium, the ratio of Mg^{2+} to Ca^{2+} in groundwater is 1. When groundwater dissolves calcite and dolomite (Equation (6)), and dissolution reaches equilibrium, the ratio of Mg^{2+} to Ca^{2+} in groundwater is close to 0.5 [30].

$$CaCO_3 + CO_2 + H_2O \rightarrow Ca^{2+} + 2HCO_3^- \quad (4)$$

$$CaMg(CO_3)_2 + 2CO_2 + 2H_2O \rightarrow Ca^{2+} + Mg^{2+} + 4HCO_3^- \quad (5)$$

$$CaCO_3 + CaMg(CO_3)_2 + 3CO_2 + 3H_2O \rightarrow 2Ca^{2+} + Mg^{2+} + 6HCO_3^- \quad (6)$$

The relationship between Mg^{2+}/Ca^{2+} and HCO_3^- in surface water and groundwater in NKWS is shown in Figure 8. All of the 37 groundwater samples were distributed in the calcite dissolution range. Surface water was uniformly distributed in calcite and dolomite dissolutions. The groundwater component in the study area was mainly dominated by the dissolution products of calcite. Meanwhile, the surface water was mainly dominated by dolomite dissolution in the rainy season and calcite dissolution in the dry season.

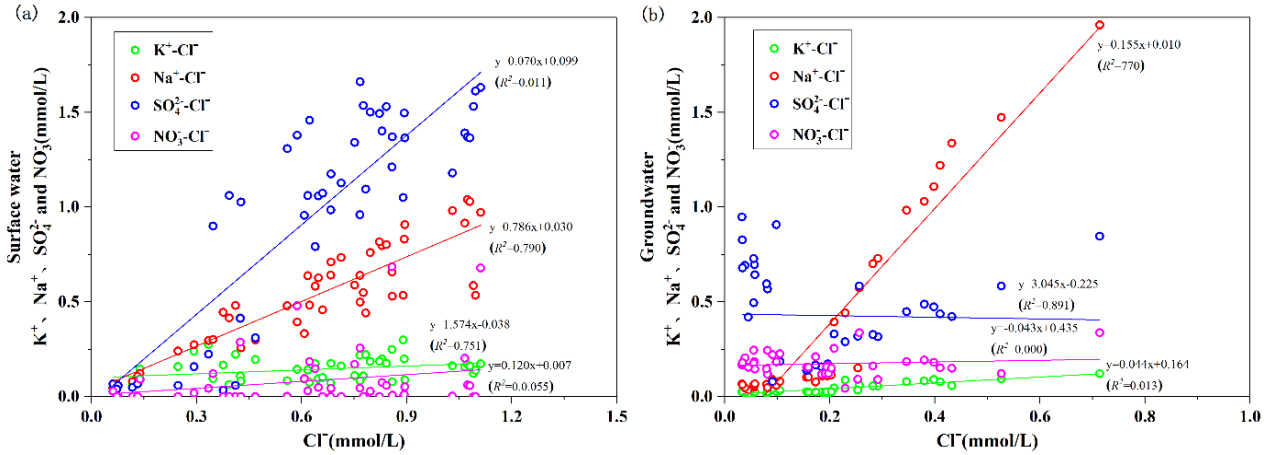

Figure 8. Relationship of Cl^- vs. K^+, Na^+, SO_4^{2-}, and NO_3^- respectively in surface water (**a**) and groundwater (**b**).

5.4. Effects of Human Activities

According to the statistical results of the chemical characteristics of precipitation in seven regions of China [31], the mass concentrations of K^+, Na^+, SO_4^{2-}, NO_3^-, and Cl^- in precipitation in southwest China were 0.675, 0.414, 10.445, 1.732, and 1.037 mg/L, respectively. The concentrations of K^+, Na^+, SO_4^{2-}, NO_3^-, and Cl^- in surface water and groundwater in the study area were higher than the local atmospheric precipitation input. Meanwhile, the concentrations of Na^+, SO_4^{2-}, NO_3^-, and Cl^- in surface water and groundwater in the study area were three times higher than those in the local precipitation. There were other important sources for these ions in water. The relationships among Cl^- and K^+, Na^+, SO_4^{2-}, and NO_3^- in surface water and groundwater in the study area were shown in Figure 9. The R^2 of the linear fits between Cl^-, and Na^+, K^+ in surface water were all greater than 0.75, indicating that Cl^- had approximately the same source as K^+ and Na^+. This result suggests that human activities, including industrial and domestic use of NaCl and agricultural fertilizers, might be the important sources for Na^+, K^+, and Cl^-. The R^2 of the linear fits among Cl^- and Na^+ and SO_4^{2-} in surface water were greater than 0.75 and are all positive. Cl^- and NO_3^- did not have a correlation.

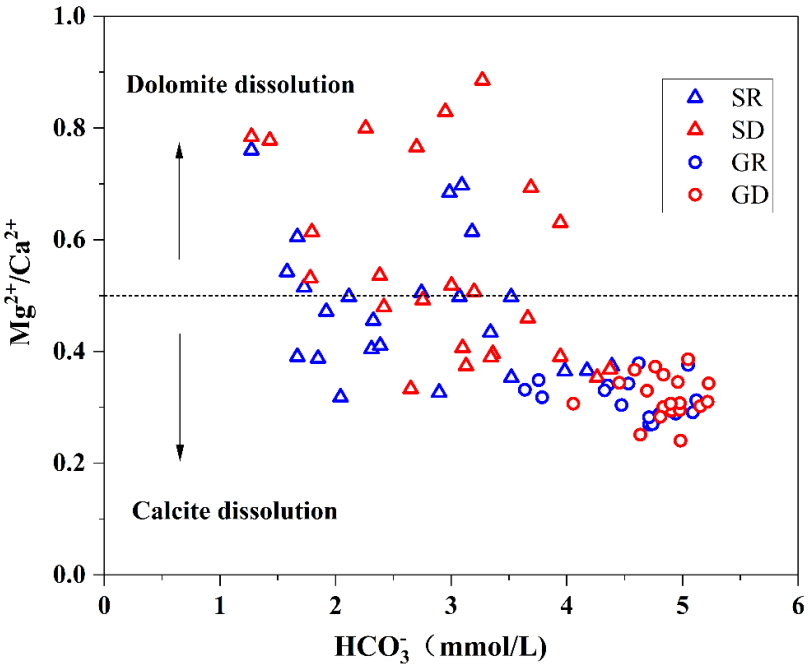

Figure 9. Relationship between HCO_3^- and Mg^{2+}/Ca^{2+}.

Na^+/Cl^- in atmospheric precipitation in southwest China was approximately 0.399 [31]. The results of this investigation showed that Na^+/Cl^- in surface water was approximately 0.540, while Na^+/C^- in groundwater was 1.236, indicating that Cl^- increased after the conversion of atmospheric precipitation into the surface water. The surface water was recharged to the groundwater through the envelope. The Na^+ and Cl^- in the water body had the same change trend, and the Cl^- concentration increased at a faster rate compared to Na^+, indicating that Na^+ and Cl^- in surface water and groundwater were influenced by atmospheric precipitation, andh uman activities. Na^+ and Cl^- in groundwater were not in balance, indicating that Na^+ may experience a cation exchange effect. The fitted relationship between K^+ and Cl^- in surface water showed that their concentrations were proportional (k = 1.574), which may be due to a common migration process during the conversion of surface water to groundwater. However, the concentration of K^+ increased relatively faster compared with Cl^-, which may be the result of potassium fertilizer application in planting. The positive relationship between Cl^- and SO_4^{2-} in groundwater suggests that precipitation was a partial source of SO_4^{2-}, which was related to the many years' acid rain in Yunnan where SO_4^{2-} was the main acidogenic factor. The fit of Cl^- to SO_4^{2-} was better than that of NO_3^-, suggesting that NO_3^- in the surface and groundwater may be more influenced by human activities than SO_4^{2-}.

The NO_3^-/Cl^- ratio is necessary to eliminate the effects of concentration or hygroscopic effects in groundwater, combined the relationship with Cl^- to identify the sources of NO_3^- in groundwater. When the amount of Cl^- is high, and that of NO_3^-/Cl^- was low, the main sources of NO_3^- in groundwater are manure and domestic sewage. When the amount of NO_3^-/Cl^- is high, and that of Cl^- was low, the main sources are chemical fertilizers [32]. Figure 10 shows that most groundwater samples in the study area were mainly distributed in the area of low Cl^- mass concentration and high NO_3^-/Cl^- ratio, indicating that NO_3^- in groundwater mainly came from chemical fertilizers. Besides, the distribution of samples was fragmented with large differences in the degree of influence by chemical fertilizers. However, the surface water samples were mainly distributed in the area of high Cl^- mass concentration and low NO_3^-/Cl^-—ratio, indicating that NO_3^- in surface water was mainly from human waste and domestic sewage.

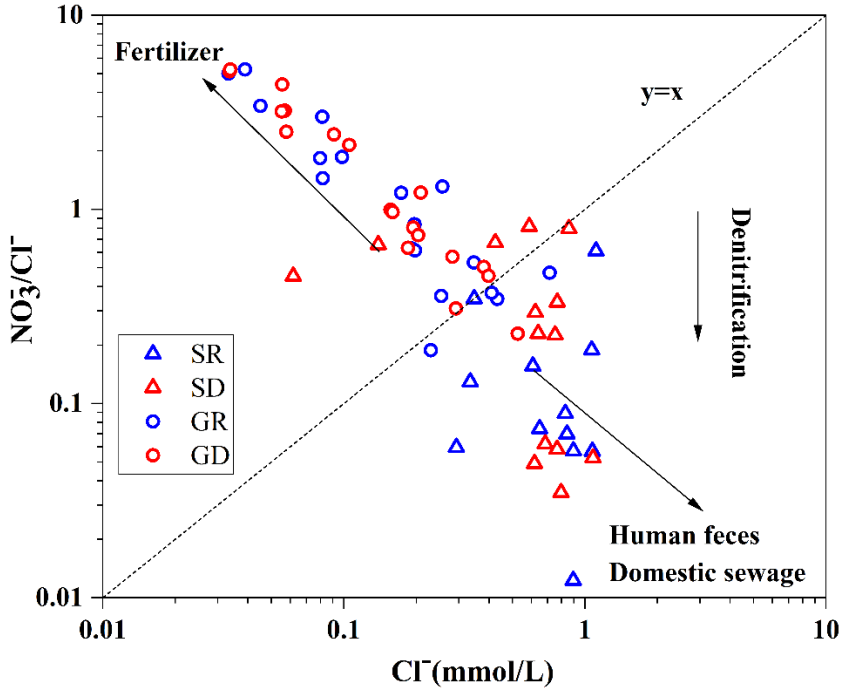

Figure 10. Relationship between Cl^- and NO_3^-/Cl^-.

6. Conclusions

This work presents a hydrogeochemical study of the NKWS with the goal of rational exploitation and sustainable utilization of water resources. The hydrochemistry characteristics and genesis of groundwater were analyzed by using certain methods, such as descriptive statistics analysis, Piper diagram, correlation analysis, and Gibbs diagram. The main conclusions are as follows:

(1) The groundwater in the NKWS were mainly weakly alkaline freshwater. The contents of major cations in groundwater in the study area were in the following order: $Ca^{2+} > Mg^{2+} > Na^+ > K^+ > NH_4^+$. The major anion contents in groundwater were in the following order: $HCO_3^- > SO_4^{2-} > NO_3^- > Cl^- > NO_2^-$. The dominant ions were Ca^{2+} and HCO_3^-. Only NH_4^+ in surface water was exceeded, and the exceedance times of NH_4^+ in the dry season were higher than those in the rainy season. The spatial variability of the NO_3^-, NO_2^-, and NH_4^+ ions in surface water and the Na^+, NO_2^-, and NH_4^+ ions in groundwater were large, and they were easily influenced by external factors. K^+, Ca^{2+}, Mg^{2+}, HCO_3^-, SO_4^{2-}, and Cl^- were the stable ions in groundwater in the study area.

(2) Controlled by the lithology of karst area, the water chemistry types of groundwater were mainly HCO_3–Ca (75.68%) and HCO_3–Ca·Mg (19.22%), and the water chemistry types of surface water in the study area were $HCO_3 \cdot SO_4$–Ca·Mg (47.92%), HCO_3–Ca·Mg (27.08%), $HCO_3 \cdot SO_4$–Ca (5.00%).

(3) The natural and anthropogenic processes contributed to the chemical composition of surface water and groundwater in the study area. However, the main factor affecting the quality of surface water and groundwater was the input of anthropogenic contaminants. In terms of natural factors, the main chemical ions of surface water and groundwater were mainly controlled by water-rock action originating from weathering and hydrolysis of rocks and soils. Ca^{2+}, Mg^{2+}, and HCO_3^- mainly originated from natural dissolution of carbonate rocks. K^+, Na^+, SO_4^{2-}, and Cl^- were partly from atmospheric precipitation. For human activities, Na^+ and Cl^- were partly from domestic water for local residents. K^+ was related to the application of potassium fertilizer. SO_4^{2-} in surface water mainly came from mining. Meanwhile, NO_3^- in surface water were mainly from human waste and domestic sewage, and NO_3^- in groundwater mainly came from chemical fertilizers.

Author Contributions: Conceptualization, Writing—original draft, Writing—review & editing, Methodology, Validation, Investigation, X.Z. Methodology, Validation, Formal analysis, Writing—review & editing, L.L. Conceptualization, Funding acquisition, Project administration, F.L. Conceptualization, J.L. Investigation, S.H. All authors have read and agreed to the published version of the manuscript.

Funding: This research was financially supported by the National Natural Science Foundation of China (No.51879085, 52170160) and the National Key Research and Development Program (No.2016YFC0502502).

Institutional Review Board Statement: Not applicable.

Informed Consent Statement: Not applicable.

Data Availability Statement: The datasets used or analyzed during the current study are available from the corresponding author upon reasonable request.

Acknowledgments: Thanks are given to Kun Qin, Zhiming Yang, and Lang Jiang for their help in field work.

Conflicts of Interest: The authors declare no conflict of interest.

References

1. Jiang, Y.; Wu, Y.; Groves, C.; Yuan, D.; Kambesis, P. Natural and Anthropogenic Factors Affecting the Groundwater Quality in the Nandong Karst Underground River System in Yunan, China. *J. Contam. Hydrol.* **2009**, *109*, 49–61. [CrossRef] [PubMed]
2. Yu, Y.; Zhao, W.; Martinez-Murillo, J.F.; Pereira, P. Loess Plateau: From Degradation to Restoration. *Sci. Total Environ.* **2020**, *738*, 140206. [CrossRef] [PubMed]
3. Wang, Z.; Yin, J.-J.; Pu, J.; Wang, P.; Liang, X.; Yang, P.; He, Q.; Gou, P.; Yuan, D. Integrated Understanding of the Critical Zone Processes in a Subtropical Karst Watershed (Qingmuguan, Southwestern China): Hydrochemical and Isotopic Constraints. *Sci. Total Environ.* **2020**, *749*, 141257. [CrossRef] [PubMed]
4. Li, C.; Gao, X.; Wang, W.; Zhang, X.; Zhang, X.; Jiang, C.; Wang, Y. Hydro-Biogeochemical Processes of Surface Water Leakage into Groundwater in Large Scale Karst Water System: A Case Study at Jinci, Northern China. *J. Hydrol.* **2020**, *596*, 125691. [CrossRef]
5. Qin, W.; Han, D.; Song, X.; Liu, S. Environmental Isotopes (Δ18O, Δ2H, 222Rn) and Hydrochemical Evidence for Understanding Rainfall-Surface Water-Groundwater Transformations in a Polluted Karst Area. *J. Hydrol.* **2021**, *592*, 125748. [CrossRef]
6. Li, Y.; Jiang, Z.; Chen, Z.; Yu, Y.; Lan, F.; Shan, Z.; Sun, Y.; Liu, P.; Tang, X.; Rodrigo-Comino, J. Anthropogenic Disturbances and Precipitation Affect Karst Sediment Discharge in the Nandong Underground River System in Yunnan, Southwest China. *Sustainability* **2020**, *12*, 3006. [CrossRef]
7. Liu, R.; Wang, J.; Zhan, H.; Chen, Z.; Li, W.; Yang, D.; Zheng, S. Influence of Thick Karst Vadose Zone on Aquifer Recharge in Karst Formations. *J. Hydrol.* **2021**, *592*, 125791. [CrossRef]
8. Parise, M.; De Waele, J.; Gutierrez, F. Current Perspectives on the Environmental Impacts and Hazards in Karst. *Environ. Geol.* **2009**, *58*, 235–237. [CrossRef]
9. Jiang, Z.; Lian, Y.; Qin, X. Rocky Desertification in Southwest China: Impacts, Causes, and Restoration. *Earth Sci. Rev.* **2014**, *132*, 1–12. [CrossRef]
10. Li, Y.; Jiang, Z.; Yu, Y.; Shan, Z.; Lan, F.; Yue, X.; Liu, P.; Gyasi-Agyei, Y.; Rodrigo-Comino, J. Evaluation of Soil Erosion and Sediment Deposition Rates by the 137Cs Fingerprinting Technique at Different Hillslope Positions on a Catchment. *Environ. Monit. Assess.* **2020**, *192*, 717. [CrossRef]
11. Lan, F.; Qin, X.; Jiang, Z.; Meng, R.; Mo, R.; Yang, S.; Wang, W.; An, S. Influences of Land Use/Land Cover on Hydrogeochemical Indexes of Karst Groundwater in the Dagouhe Basin, Southwest China: Influences of Land Use/Land Cover on Underground Hydrogeochemistry. *Clean Soil Air Water* **2015**, *43*, 683–689. [CrossRef]
12. Helena, B. Temporal Evolution of Groundwater Composition in an Alluvial Aquifer (Pisuerga River, Spain) by Principal Component Analysis. *Water Res.* **2000**, *34*, 807–816. [CrossRef]
13. Luo, F.; Wu, G.; Wang, C.; Zhang, L. Application of Nemerow pollution index method and Single factor evaluation method in water quality evaluation. *Environ. Sustain. Dev.* **2016**, *41*, 87–89, (In Chinese with English Abstract). [CrossRef]
14. Miao, Q.; Li, X.; Xu, Y.; Liu, C.; Lv, Z. Chemical Characteristics of Groundwater and Source Identification in a Coastal City. *PLoS ONE* **2021**, *16*, e0256360. [CrossRef] [PubMed]
15. Aiuppa, A.; Bellomo, S.; Brusca, L.; D'Alessandro, W.; Federico, C. Natural and Anthropogenic Factors Affecting Groundwater Quality of an Active Volcano (Mt. Etna, Italy). *Appl. Geochem.* **2003**, *18*, 863–882. [CrossRef]
16. Brenot, A.; Baran, N.; Petelet-Giraud, E.; Négrel, P. Interaction between Different Water Bodies in a Small Catchment in the Paris Basin (Brévilles, France): Tracing of Multiple Sr Sources through Sr Isotopes Coupled with Mg/Sr and Ca/Sr Ratios. *Appl. Geochem.* **2008**, *23*, 58–75. [CrossRef]
17. Edmunds, W.M.; Shand, P.; Hart, P.; Ward, R.S. The Natural (Baseline) Quality of Groundwater: A UK Pilot Study. *Sci. Total Environ.* **2003**, *310*, 25–35. [CrossRef]

18. Valdes, D.; Dupont, J.-P.; Laignel, B.; Ogier, S.; Leboulanger, T.; Mahler, B.J. A Spatial Analysis of Structural Controls on Karst Groundwater Geochemistry at a Regional Scale. *J. Hydrol.* **2007**, *340*, 244–255. [CrossRef]
19. Négrel, P. Geochemical Study of a Granitic Area—The Margeride Mountains, France: Chemical Element Behavior and 87Sr/86Sr Constraints. *Aquat. Geochem.* **1999**, *5*, 125–165. [CrossRef]
20. Böhlke, J.K.; Horan, M. Strontium Isotope Geochemistry of Groundwaters and Streams Affected by Agriculture, Locust Grove, MD. *Appl. Geochem.* **2000**, *15*, 599–609. [CrossRef]
21. Petelet-Giraud, E.; Négrel, P.; Casanova, J. Variability of ^{87} Sr/ ^{86} Sr in Water Draining Granite Revealed after a Double Correction for Atmospheric and Anthropogenic Inputs. *Hydrol. Sci. J.* **2003**, *48*, 729–742. [CrossRef]
22. Widory, D.; Kloppmann, W.; Chery, L.; Bonnin, J.; Rochdi, H.; Guinamant, J.-L. Nitrate in Groundwater: An Isotopic Multi-Tracer Approach. *J. Contam. Hydrol.* **2004**, *72*, 165–188. [CrossRef] [PubMed]
23. Négrel, P.; Petelet-Giraud, E. Strontium Isotopes as Tracers of Groundwater-Induced Floods: The Somme Case Study (France). *J. Hydrol.* **2005**, *305*, 99–119. [CrossRef]
24. Zhu, X.; Fan, T.; Guan, W. The analysis of stable isotopes of precipitation in Kunming. *Yunnan Geogr. Environ. Res.* **2013**, *25*, 90–95. (In Chinese with English Abstract)
25. Tang, C.; Zheng, X.; Liang, Y. Hydrochemical Characteristics and Formation Causes of Ground Karst Water Systems in the Longzici Spring Catchment. *Environ. Sci.* **2020**, *41*, 2087–2095, (In Chinese with English Abstract). [CrossRef]
26. Feth, J.H.; Gibbs, R.J. Mechanisms Controlling World Water Chemistry: Evaporation-Crystallization Process. *Science* **1971**, *172*, 870–872. [CrossRef]
27. Gibbs, R.J. Mechanisms Controlling World Water Chemistry. *Sci. New Ser.* **1970**, *170*, 1088–1090. [CrossRef]
28. Lv, J.; An, Y.; Wu, Q.; Luo, J.; Jiang, H. Hydrochemical Characteristics and Sources of Qingshuijiang River Basin at Wet Season in Guizhou Province. *Environ. Sci.* **2015**, *36*, 1565–1572, (In Chinese with English Abstract). [CrossRef]
29. Wu, Q.; Han, G.; Tao, F.; Tang, Y. Chemical Characterization of Rainwater in a Karst Rural Site: A Case Study of Puding, China. *Environ. Sci.* **2011**, *32*, 26–32, (In Chinese with English Abstract). [CrossRef]
30. Zhou, J.; Jiang, Z.; Xu, G.; Qin, X.; Huang, Q.; Zhang, L. Major Ionic Characteristics and Controlling Factors of Karst Groundwater at Xiangshui, Chongzuo. *Environ. Sci.* **2019**, *40*, 2143–2151, (In Chinese with English Abstract). [CrossRef]
31. Xie, N.; Xue, L. The Spatial Differences of Chemical Characteristics of Precipitation in Seven Regions of China. *Hubei Agric. Sci.* **2012**, *51*, 2971–2975, (In Chinese with English Abstract). [CrossRef]
32. Puig, R.; Soler, A.; Widory, D.; Mas-Pla, J.; Domènech, C.; Otero, N. Characterizing Sources and Natural Attenuation of Nitrate Contamination in the Baix Ter Aquifer System (NE Spain) Using a Multi-Isotope Approach. *Sci. Total Environ.* **2017**, *580*, 518–532. [CrossRef] [PubMed]